

BOND-SLIP BEHAVIOR OF LONGITUDINAL REINFORCING BARS CONFINED WITH FRP SHEETS

Susumu KONO¹, Kazunari MATSUNO² And Tetsuzo KAKU³

SUMMARY

Forty cantilever type specimens were tested with and without fiber reinforced polymer (FRP) sheet confinement in order to study the improvement in bond-slip behaviors of longitudinal reinforcing bars. The FRP sheets used were carbon and aramid with the elastic modulus of 230 GPa and 118 GPa, respectively. Other variables were the amount of FRP sheet (up to 0.32%), the number (2 or 4 bars) and the diameter (19 mm or 25 mm) of longitudinal bars, and the cover depth (40mm, 57 mm, or 72 mm). Concrete strength used in the test was under 30 MPa so that the test results can be applied when retrofitting existing ordinary structures. In previous work which used the test results of twenty cantilever type specimens conducted in 1998, it was shown that the confinement greatly enhanced the bond strength and ductility, and the bond strength contribution from FRP sheet increased linearly with the elastic modulus of FRP sheet. Based on these findings, an equation was proposed to predict the bond strength for members confined with FRP sheet [5]. Test results of additional twenty specimens in 1999 showed that effectiveness of the confinement on the bond strength did not stay constant but decreased as the amount of FRP sheet increased. To take into account this new finding, a previously proposed equation was modified to make a better prediction for the bond strength. The proposed equation was validated using test results of beam and column specimens.

INTRODUCTION

It is well known that the confinement by FRP sheets greatly increases the shear capacity of reinforced concrete beams and columns. The increase in shear capacity due to FRP sheets has been experimentally evaluated and incorporated in design equations [1] in 1990's. According to a truss analogy, the increase in shear capacity also increases the demand on bond stress. However, the increase in bond strength for members confined with FRP sheets has not been quantified. In 1998, twenty cantilever type specimens and four beam specimens were tested in Toyohashi University of Technology to study the increase in bond strength for members confined with FRP sheets [5]. It was reported that the bond strength increased linearly with the elastic modulus and the amount of FRP sheets but was independent of the depth and number of longitudinal bars. Based on those observations, a design equation was proposed to predict the increase in bond strength due to FRP sheets confinement. In 1999, additional twenty cantilever type specimens were tested in order to investigate the effects of the amount and elastic modulus of FRP sheets on the bond behavior. Similar to the test results in 1998, the bond strength increased linearly with the elastic modulus of FRP sheets. In addition, it was found that the effectiveness of FRP sheet on the bond strength did not stay constant but decreased as the amount of FRP sheet increased. In this study, the test results of total forty cantilever type specimens are summarized and a modified design

equation for the bond strength is proposed. The proposed equation is validated using test results of beam and column specimens.

¹ Dept. of Architecture, Kyoto University, Kyoto, Japan Email:Kono@archi.kyoto-u.ac.jp

² Kure National College of Technology, Hiroshima, Japan Email: Matuno@kure-nct.ac.jp

³ Dept. of Civil Eng., Toyohashi University of Technology, Toyohashi, Japan Email:Kaku@jughead.tutrp.tut.ac.jp

EXPERIMENTAL PROGRAM

Test specimens

Shown in Fig. 1(a) is the cantilever type specimen used in this study. The specimen shown in a solid line is considered to be a half of a fictitious simply supported beam specimen shown in a break line. The term 'cantilever' came from the fact that the half of the simply support beam is equivalent to a cantilever beam. The upper two or four longitudinal bars were directly pulled as tension reinforcement of a fictitious beam. The bond length was 300 mm and the right 100 mm end was encased in a steel pipe to prevent bond with the surrounding concrete. Two closed $\phi 6$ bars were placed around the longitudinal bars as shear reinforcement of 0.186% as shown in Fig. 1(b). These shear and longitudinal bars formed the main reinforcement. Supplemental reinforcement made from D10 and D19 bars (D: deformed, 10 & 19: nominal bar diameter in mm), solid lines in Fig. 1(a), was placed inside the main reinforcement to avoid a shear failure. Without FRP confinement the specimen was designed to fail in the side split mode according to the design equation of Fujii and Morita[2]. Sheet arrangements are shown in Fig. 1(c). One layer of FRP sheet in this configuration corresponds to ρ_{wf} of 0.08%. For other amount of ρ_{wf} , multiple layers of FRP sheets were used.

Table 1: Mechanical Properties of Concrete

Batch Number	f'_c (MPa)	f_t (MPa)	E_c (GPa)
Batch1	29.4	2.70	24.7
Batch2	24.5	1.65	20.9
Batch3	27.0	2.43	20.1

Table 2: Mechanical Properties of Steel

Reinforcement	f_y (MPa)	f_u (MPa)	E_s (GPa)
D25	703	889	192
D19	720	840	200
D10	368	525	179
$\phi 6$ for Batch1	272	397	197
$\phi 6$ for Batch2	277	414	173
$\phi 6$ for Batch3	269	410	171

Table 3: Mechanical Properties of FRP sheet

	Carbon	Aramid
Weight per unit area (gram/m ²)	300	415
Density(gram/m ³)	1.8	1.45
Design thickness(mm)	0.167	0.286
Nominal Tensile strength(MPa)	3400	2000
Nominal Elastic Modulus(GPa)	230	118
Tensile strain at fracture (%)	1.50	1.80

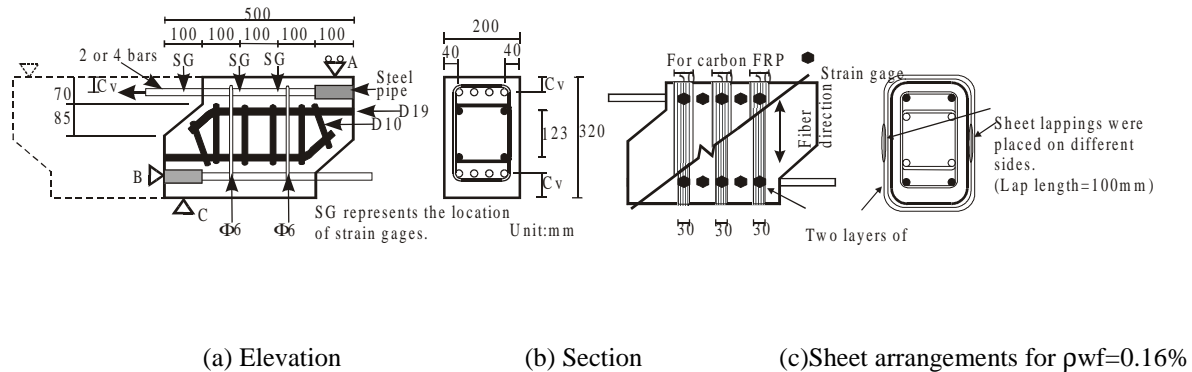


Figure 1: Specimen dimensions

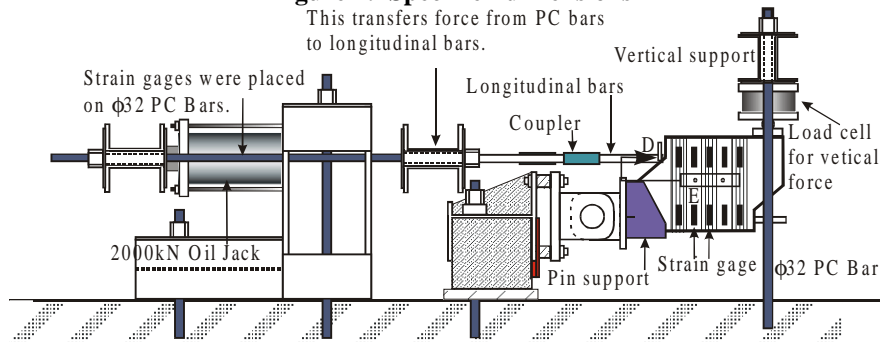


Figure 2: Loading system

The mechanical properties of the concrete and reinforcement are shown in Tables 1 and 2, and those of the FRP sheets are shown in Table 3. The mix proportions by weight for Batches 1 and 2 were 0.63: 1.00: 3.06: 3.55

(water: cement: fine aggregate: coarse aggregate) and that for Batch 3 was 0.63: 1.00: 3.01: 3.42. The maximum aggregate size was 20 mm. Forty cantilever specimens were prepared that included five test variables: the vertical cover, Cv, the diameter and the number of longitudinal bars, and the type and the amount of FRP sheets. The test variables for all cantilever type specimens are shown in Table 4. Specimens C1 through C20 were tested in 1998 and Specimens C21 through C40 in 1999.

Test setup and procedures

The loading system for cantilever specimens is shown in Fig. 2. Strains in the FRP sheets and concrete surface were measured at ten locations on one side of the specimen. Strains in each longitudinal bar were also measured at three locations as shown in Fig. 1(a). After testing of the upper longitudinal bars was completed, the lower longitudinal bars were tested by rotating a specimen by 180 degrees. Since strains on the lower FRP sheet surface were less than 0.02% while the upper longitudinal bars were tested, the confinement by sheets was assumed to be identical for the upper and the lower bars.

Table 4: Test Variables for Specimens

Specimen		Variables							Results		
Type	Number	Longitudinal bar				FRP		Concrete	Bond strength τ_{exp} *4 (MPa)	Mode of failure*5	α *6
		Location at casting*1	Vertical cover Cv (mm)	Nominal diameter db (mm)	Number of bars	Type of sheet*2	Sheet ratio*3 ρ_{wf} (%)	f'c (MPa)			
Batch1	C1	T	40	19	2	C	0	29.4	5.08	C	N/A
	C2	B	57						6.02	S	N/A
	C3	T	40						6.43	CS	3.12(C1)
	C4	B	57						7.11	S	2.49(C2)
	C5	T	40						2.54	S	N/A
	C6	B	57		3.00		S		N/A		
	C7	T	40		4		0.16		3.90	S	6.32(C5)
	C8	B	57						4.31	S	6.01(C6)
	C9	T	40						3.39	S	2.50(C5)
	C10	B	57						3.78	S	2.29(C6)
C11	T	72	25	2		A		0.16	24.5	5.67	S
C12	B	57			4.31		S			N/A	
C13	T	72			6.71		S			2.65(C11)	
C14	B	57			5.33		S			3.39(C12)	
C15	T	40			3.11		S			N/A	
C16	B	40			4.02		CS			N/A	
C17	T	40			5.28		S			4.20(C16)	
C18	B	40			4.90		S			2.90(C16)	
C19	T	40			5.38		C			1.89(C1)	
C20	B	57			5.64		S			0.34(C2)	
Batch3	C21	T	40	19	4	C	0	27.0	*7	*7	N/A
	C22	B							2.47	Sh	N/A
	C23	T							4.78	Sh	N/A
	C24	B							2.58	S	N/A
	C25	T							4.51	C	N/A
	C26	B							2.67	Sh	N/A
	C27	T							5.22	CS	2.77(*a)
	C28	B							3.03	S	4.36(*b)
	C29	T							5.32	CS	3.26(*a)
	C30	B							3.24	CS	6.36(*b)
	C31	T			5.42		S		1.87(*a)		
	C32	B			3.22		C		3.11(*b)		
	C33	T			5.42		CS		1.20(*a)		
	C34	B			3.75		S		3.61(*b)		
	C35	T			6.20		S		1.87(*a)		
	C36	B			3.79		S*7		(2.92(*b))		
	C37	T			5.52		C		4.23(*a)		
	C38	B			2.89		S		3.02(*b)		
	C39	T			5.05		C		0.98(*a)		
	C40	B			3.00		S		2.05(*b)		

*1: T and B represent top and bottom, respectively. *2: C and A represent carbon and aramid, respectively. *3: the fiber area ratio calculated in the same manner with shear reinforcement *4: Values for upper bars have been normalized for lower bars by multiplying 1.22. *5: C: corner and side split failure S:side split failure Sh:shear failure. *6: Magnification factor for FRP sheets. *7: Loading system did not work for C20. C36 failed outside the test region and higher capacity is expected. *a is the average bond strength of C23 and C25, *b is the average bond strength of C22, C24, and C26.

TEST RESULTS AND DISCUSSION

Load-displacement relations

Defining slip as the relative horizontal displacement between D and E in Fig. 2, total tensile force and slip relations for selected cantilever specimens are shown in Fig. 3. They have different amount of FRP confinement but are identical otherwise. Numbers in parentheses next to the specimen designation indicate ρ_{wf} . From Fig. 3, it can be seen that the bond strength, the peak slip, and the energy consumed by the peak increased as ρ_{wf} increased. It is clear that the confinement greatly enhanced the ductility.

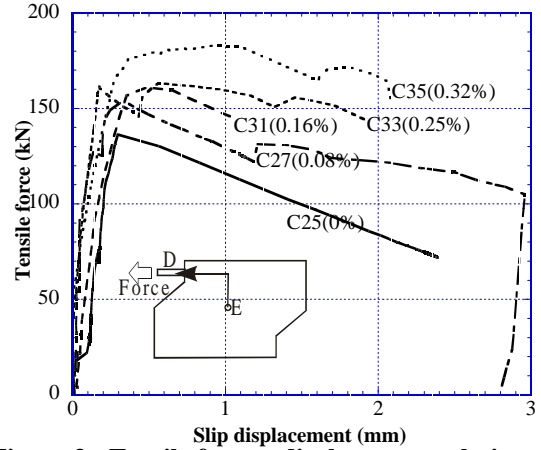


Figure 3: Tensile force – displacement relations

Failure modes

Although all cantilever specimens were designed to fail in a side split mode without FRP sheets, failure modes varied as shown in Table 4. Fig. 4 shows crack patterns and failure modes of representative specimens with different amount of FRP sheet. Only the upper half of the specimen is schematically shown. Without any confinement, failure modes were a mixture of corner and side split failure or a brittle shear failure. With confinement of $\rho_{wf}=0.16\%$, a shear failure changed to a corner split failure and a mixed mode to a side split failure. With additional 0.16% confinement, failure modes became side split failures. As confinement increased, the number of cracks increased over the wide range of surface and each crack size became smaller. The large amount of increase in bond strength can be attributed to this damage distribution which necessitated a large amount of energy consumption.

	$\rho_{wf}=0\%$	$\rho_{wf}=0.16\%$	$\rho_{wf}=0.32\%$
2 bars	 C25 Corner and side split	 C31 Side split $\tau_{exp} + 21$	 C35 Side split $\tau_{exp} + 14$
4 bars	 C22 Shear	 C32 Corner $\tau_{exp} + 31$	 C36 Side split $\tau_{exp} + 18$

Figure 4: Crack patterns and failure modes

Increase in bond strength due to FRP confinement

It is well known that the bar location at casting greatly affects the bond strength, and hence the bond strength for upper and lower bars cannot be directly compared. For this the bond strengths for the upper bars were multiplied by 1.22 to normalize their results with respect to strengths for lower bars and those normalized strength, τ_{exp} , is listed in Table 4. The loading system did not work properly for C21 and data was not taken. C30 failed outside the test region and the maximum shear before this premature failure is listed in the table.

Equation 1 defines the increase of bond strength, $\Delta\tau_{exp}$, due to confinement.

$$\Delta\tau_{exp} = \tau_{exp}(confined) - \tau_{exp}(prototype) \quad (1)$$

The bond strength contribution, τ_{wf} , from FRP sheet confinement is tentatively expressed by Eq. 2 which has a similar format to that of bond strength contribution from shear reinforcement proposed by Fujii and Morita [2].

$$\tau_{wf} = \alpha \cdot \left(9.51 \frac{\rho_{wf} \cdot b}{N \cdot d_b} \right) \cdot \sqrt{f'c} \quad (\text{MPa}) \quad (2)$$

where α is a factor to be determined, ρ_{wf} the fiber ratio calculated in the same manner with shear reinforcement, b the width of a beam, N the number of longitudinal bars, and d_b the diameter of longitudinal bars. Since it is impossible to isolate the effect of sheet confinement on the bond strength, the increase of bond strength, $\Delta\tau_{\max}$, defined by Eq. 1 is assumed to be totally due to FRP sheet confinement. Equating $\Delta\tau_{\exp}$ to τ_{wf} , a magnification factor, α , is computed for each specimen as shown in Table 4 with the unconfined companion specimen number in parentheses. Figure 5 shows the influence of three variables on α . Similar to the results in Ref. 5, the top cover depth and the bar diameter did not have much influence on α and they are not discussed here. From Figs. 5(a) and (b), it can be seen that α increases linearly with the number of longitudinal bars and the elastic modulus of FRP sheet. Based on these facts α was determined and Eq. 2 was expressed as Eq. 3 in Ref. 5.

$$\tau_{wf} = \left(\frac{E_{wf}}{E_o} + 0.5 \right) \cdot \left(9.51 \frac{\rho_{wf} \cdot b}{d_b} \right) \cdot \sqrt{f'c} \quad (\text{MPa}) \quad (3)$$

where $E_o=230000\text{MPa}$. New test results (C21- C40) in Fig. 5(c) show that α decreases with increasing ρ_{wf} , that is, FRP sheets become less effective in increasing the bond strength as ρ_{wf} increases.

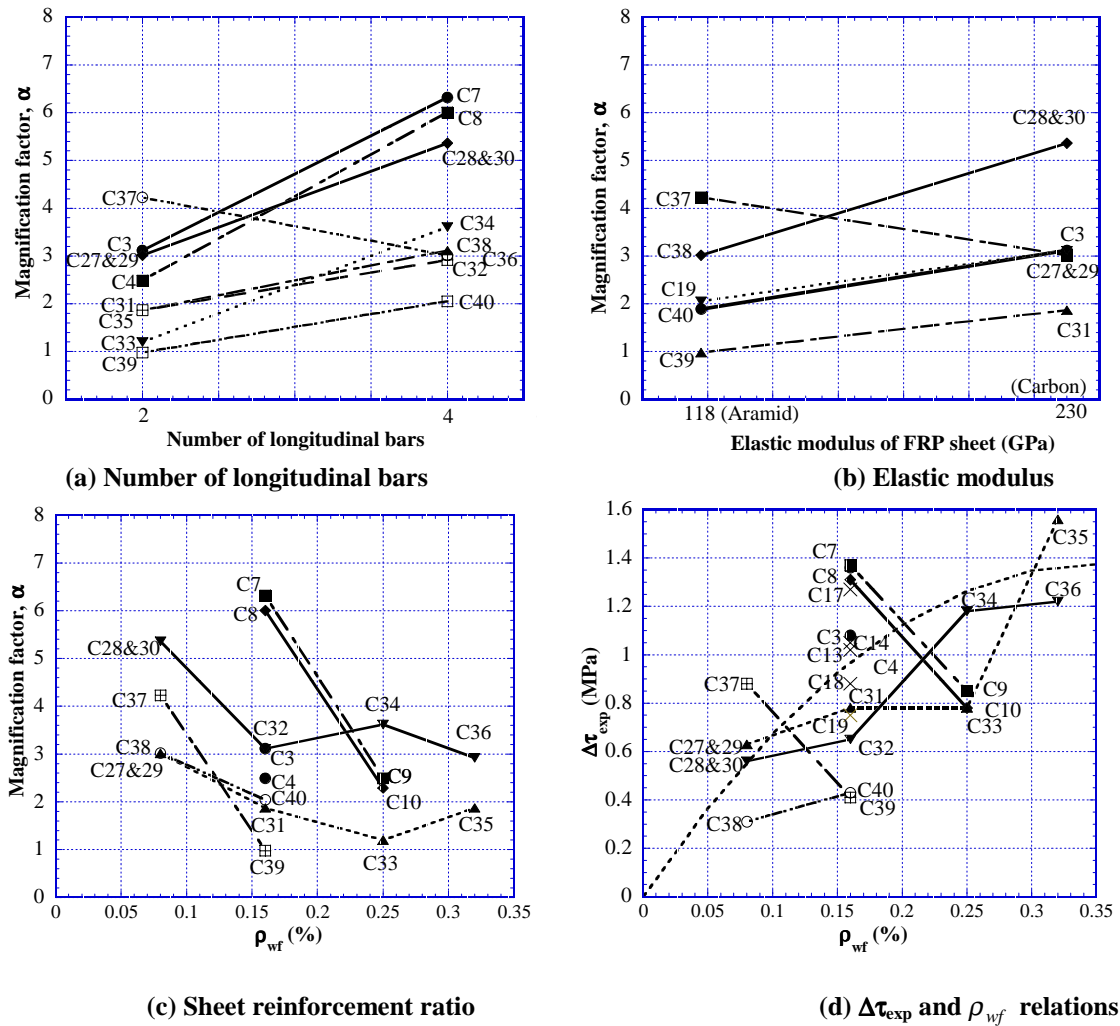


Figure 5: Effects of test variables on α and $\tau_{wf} - \rho_{wf}$ relations

This is clear from $\Delta\tau_{\text{exp}} - \rho_{\text{wf}}$ relations shown in Fig. 5(d). Studying changes in $\Delta\tau_{\text{exp}}$ for a set of C27, C29, C31, C33, and C35 or a set of C28, C30, C32, C34, and C36, the relation between $\Delta\tau_{\text{exp}}$ and ρ_{wf} may be more appropriately expressed by a parabolic function as shown by a dotted line in Fig. 5(d) rather than the linear relation between τ_{wf} and ρ_{wf} seen in Eq. 3. This parabolic function was determined so that (1) the curve passes the origin and (2) ρ_{wf} for the peak of the curve is 0.35%. Since a parabola has three degrees of freedom, one more criterion gives the exact shape of the parabola. The last criterion was that the average of predicted τ_{wf} for specimens in Table 4 matched the average of experimental values for $\Delta\tau_{\text{exp}}$. In this manner, Eq. 3 was modified as Eq. 4.

$$\tau_{\text{wf}} = 0.01118 \cdot \left(\frac{E_{\text{wf}}}{E_o} + 0.5 \right) \cdot \left(\frac{b}{d_b} \right) \cdot \left\{ -\frac{1.5}{0.0035^2} \cdot (\rho_{\text{wf}} - 0.0035)^2 + 1.5 \right\} \cdot \sqrt{f'c} \quad (\text{MPa}) \quad (4)$$

Equation 4 is then simplified as Eq. 5.

$$\tau_{\text{wf}} \approx \frac{1}{60} \cdot \left(\frac{E_{\text{wf}}}{E_o} + 0.5 \right) \cdot \left(\frac{b}{d_b} \right) \cdot \left[1 - \left(\frac{\rho_{\text{wf}}}{0.0035} - 1 \right)^2 \right] \cdot \sqrt{f'c} \quad (\text{MPa}) \quad (5)$$

Values τ_{wf} computed by Eq. 5 are compared with $\Delta\tau_{\text{exp}}$ in Fig. 6(a). The average of $\Delta\tau_{\text{exp}}/\tau_{\text{wf}}$ was 1.01 with a standard deviation of 0.32. The average was not equal to 1.00 because of a round off in Eq. 5.

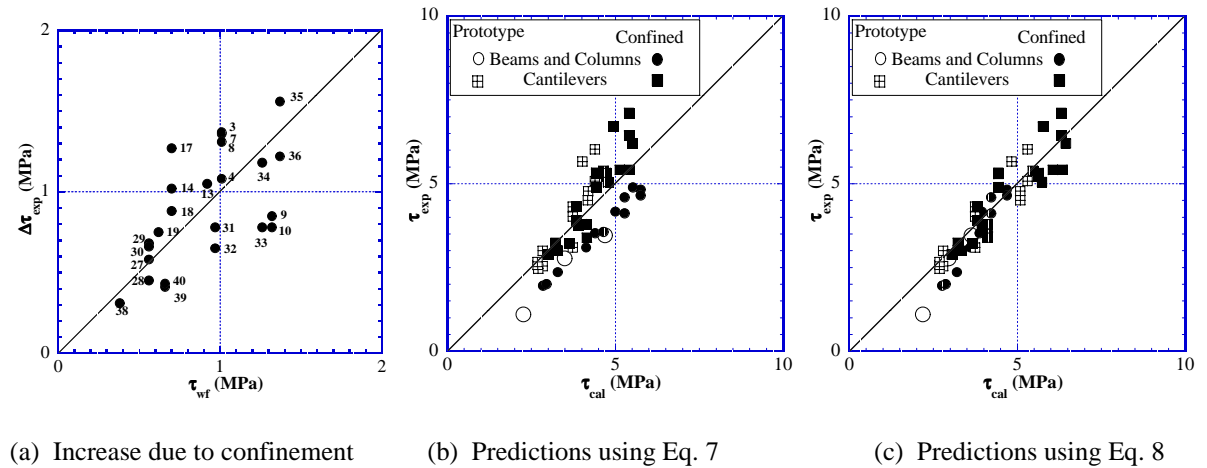


Figure 6: Comparison between computed and experimental bond strengths

To compute the total bond strength, the bond contribution from FRP sheets, τ_{wf} , needs to be added to the bond contribution from concrete and shear reinforcement. Here, equations by Orangun et al.[3] (OJB equation) and Fujii and Morita[2] (FM equation) for side split failure are used. They are expressed in MPa unit as follows.

$$\tau_{\text{cal}}^{\text{OJB}} (\text{unconfined}) = \left[0.0996 + 0.249 \frac{C}{d_b} + 4.15 \frac{d_b}{l_s} + 0.0241 \frac{\rho_{\text{ws}} \cdot b \cdot f_{\text{ys}}}{N \cdot d_b} \right] \sqrt{f'c} \quad (5)$$

$$\tau_{\text{cal}}^{\text{FM}} (\text{unconfined}) = \left[0.117 \cdot \left(\frac{b}{N \cdot d_b} - 1 \right) + 0.163 + 9.51 \frac{\rho_{\text{ws}} \cdot b}{N \cdot d_b} \right] \sqrt{f'c} \quad (6)$$

where C is the smaller of the clear bottom cover or half the clear spacing between the next adjacent bar, d_b the diameter of the longitudinal bars, ρ_{ws} the shear reinforcement ratio, f_{ys} the yield strength of transverse reinforcement, b the width of a beam, and N the number of longitudinal bars. Since the original FM equation was defined for upper bars the factor of 1.22 was used to obtain Eq. 6 for lower bars. The predictions by Eq. 5 and 6 had errors for the fourteen unconfined cantilever specimens. Since it is not the purpose of this study to

discuss the validity of OJB and FM equations, factors of 0.98 for OJB equation and 1.30 for FM equation were used respectively to match the bond strength for the 14 unconfined cantilever specimens. The final form of the bond strength is then expressed as follows.

$$\tau_{cal}^{OJB} = \lambda_{OJB} \cdot \tau_{cal}^{OJB} (unconfined) + \tau_{wf} \quad (\text{MPa}) \quad (7)$$

$$\tau_{cal}^{FM} = \lambda_{FM} \cdot \tau_{cal}^{FM} (unconfined) + \tau_{wf} \quad (\text{MPa}) \quad (8)$$

where $\lambda_{OJB}=0.98$ and $\lambda_{FM}=1.30$ for cantilever specimens and 1.0 for beams and columns. In Figs. 6(b) and (c), τ_{cal}^{OJB} and τ_{cal}^{FM} are compared with τ_{exp} for 17 unconfined specimens and 36 confined specimens. Specimens include beam and cantilever specimens tested in Toyohashi University of Technology and column specimens in References 4 and 6. Since the figure shows that predictions by FM equation is slightly better than OJB equation, it is recommended that the bond strength for beams and columns confined with FRP sheets be predicted using the following equation.

$$\tau_{cal}^{FM} (confined) = \left[0.117 \cdot \left(\frac{b}{N \cdot d_b} - 1 \right) + 0.163 + 9.51 \frac{\rho_{ws} \cdot b}{N \cdot d_b} + \frac{1}{60} \cdot \left(\frac{E_{wf}}{E_o} + 0.5 \right) \cdot \left(\frac{b}{d_b} \right) \cdot \left[1 - \left(\frac{\rho_{wf}}{0.0035} - 1 \right)^2 \right] \right] \sqrt{f'_c} \quad (\text{MPa}) \quad (9)$$

Equation 9 gives reasonable results as long as the bond strength of an unconfined prototype specimen is evaluated properly. At this point, it is not clear if τ_{wf} stays constant with the number of longitudinal bars more than four and it is safer to assume that the maximum bond force is limited to 4 times τ_{wf} times the bond area per bar. Value ρ_{wf} greater than 0.35% should be also neglected and computed as $\rho_{wf} = 0.35\%$ since there is no data. It is also noted that Eq. 9 has not been checked for concrete strength greater than 30MPa.

It is interesting that the bond contributions from shear reinforcement and FRP sheet do not necessarily have a same format in terms of the number of longitudinal bars, and the amount and the elastic modulus of shear reinforcement or FRP sheets. If shear reinforcement and FRP sheets work similarly as tension cords in a truss mechanism, they are supposed to have a similar format. Hence, it is still necessary to clarify the shear transfer mechanisms and explain the meaning for each term in the proposed equation.

CONCLUSIONS

From test results on forty cantilever type specimens, the confining effects of FRP sheets on bond slip behavior were evaluated.

1. The confinement greatly increased the bond strength and ductility. These effects were confirmed by comparing load-slip relations and the crack patterns for specimens with different amount of confinements.
2. The bond strength contribution due to FRP sheet increased linearly with increasing elastic modulus of FRP sheet. The number of longitudinal bars had no influence on the bond strength. These results confirmed the conclusions previously obtained for the first twenty cantilever type specimens.
3. The effectiveness of FRP sheets on the increase in bond strength decreased as the amount of FRP sheet increased. Based on this new finding, a previously proposed equation to predict the increase in bond strength due to FRP confinement was modified. As long as the bond strength of an unconfined prototype specimen is evaluated properly, the bond strength of confined specimens can be predicted accurately

ACKNOWLEDGEMENTS-

The authors acknowledge the financial support provided by the Association of SR-CF Engineering and thank graduate students at Toyohashi University of Technology including Ms. Obata, Ms. Yamazaki, and Mr. Okamura for providing assistance in experiments and data analyses.

REFERENCES

1. Architecture Institute of Japan (1998), 'Applications of fiber reinforced plastics to concrete structures,' AIJ-9809-01000, pp. 88-91.
2. Fujii, S. and Morita, S. (1982), 'Splitting Bond Capacities of Deformed Bars, Part2 A proposed ultimate strength equation for splitting bond failure,' *Journal of Structural and Construction Engineering*, Architectural Institute of Japan, Vol. 319, pp. 47-55, Nov.
3. Orangun, C.O., Jirsa, J.O. and Breen, J.E. (1977), 'A Reevaluation of Test Data on Development Length and Splices,' *ACI Journal*, Proc., Vol. 74, No. 3, March, pp. 114-122; Discussion, pp. 470-475.
4. Katsumata, H., Kobatake, Y., Takeda, T. (1987), 'A Study of Strengthening with Earthquake-Resistant Capacity of Existing Reinforced Concrete Columns, (Part 2) -Tests on Strengthening Square-Sectioned Columns-,' *Report of Research Institute*, Obayashi Construction, No.34, pp. 114-118.
5. Kono, S., Matsuno, S., and Kaku, T. (1999), "Experimental Study on Bond-Slip Behavior of Longitudinal Bars in RC Beams Confined with FRP Sheets," *Fourth International Symposium on Fiber Reinforced Polymer for Reinforced Concrete Structures*, Baltimore, October.
6. Hagio, H., Katsumata, H., Kobatake, Y. (1997), 'Seismic Retrofitting of Existing Reinforced Concrete Columns with Carbon Fibers (Part 3 Experimental Study of Bond Splitting Failure of Retrofitted Columns),' *Summaries of technical papers of annual meeting*, Architectural Institute of Japan, Vol. C-2, pp. 669-670.